

# Small Signal Analysis of Active Clamp Flyback Converters in Transition Mode and Burst Mode

Pei-Hsin Liu  
Texas Instruments  
Manchester, NH USA  
p-liu@ti.com

**Abstract**—Active clamp flyback (ACF) converters in transition mode improves the full load efficiency of high-frequency AC/DC and DC/DC power supplies with zero-voltage switching (ZVS). To minimize the impact of the circulating energy for ZVS, burst mode control is used to benefit ACF light load efficiency. However, due to the resonance nature of ACF switching current waveforms, it is difficult to characterize the small-signal properties analytically. In this paper, two new small signal models are developed, and analytical design guides are investigated. An average modeling technique for the transition mode ACF is developed which eliminates the complexity of describing the second-order resonance waveforms, and the model enables a higher system bandwidth design. A high-frequency model for burst mode is derived with the describing function method, which identifies the loop compensation impact and differentiates the stability criteria from the conventional ripple-based ( $V^2$ ) control. Enlightened from the models, a novel nonlinear ramp compensation method and a parallel damping technique are proposed to improve the loop stability and optimize the dynamic response. Finally, SIMPLIS simulations verify the model accuracy, and the fast transient response with the compensation methods are demonstrated on a high-density 45W GaN ACF notebook adapter.

**Keywords**—Active clamp Flyback; transition mode; burst mode; small signal model; ramp compensation

## I. INTRODUCTION

Active clamp flyback converter (ACF) provides greater efficiency at a higher switching frequency ( $f_{sw}$ ) than the conventional flyback converters, because of zero voltage switching (ZVS) and recycling the leakage energy of the transformer to output [1][2][3]. Besides, the transition mode (TM) operation obtains ZVS across a wider operating range than the continuous conduction mode (CCM) by fully utilizing the magnetizing energy of the transformer [4][5][6]. As the high-side switch ( $Q_H$ ) of ACF conducts, the magnetizing current ( $I_M$ ) can change in a reverse direction in TM. After  $Q_H$  turns off, the negative magnetizing current ( $I_{M(-)}$ ) is used to discharge the switch-node capacitance ( $C_{sw}$ ), so the switch-node voltage ( $V_{sw}$ ) can transient to 0V before  $Q_L$  turns on. Even though the widely used constant-frequency peak current control may allow ACF running in TM at a higher input bulk-capacitor voltage ( $V_{BULK}$ ) conditions, the efficiency at a lower  $V_{BULK}$  and/or a lower output voltage ( $V_O$ ) conditions impairs due to losing  $I_{M(-)}$  in CCM. Moreover, the subharmonic oscillation issue and the phase delay effect of right-half-plane (RHP) zero in CCM complicates the control loop designs and limits the outer-loop control bandwidth [7].

Instead, the variable-frequency hysteresis current-mode control of UCC28780 resolves those issues, since the additional emulated valley current loop independently controls  $I_{M(-)}$  to prevent ACF from entering into CCM. The block diagram and switching waveforms are illustrated in Fig. 1 [8]. The peak current loop controls the peak magnetizing current ( $I_{M(+)}$ ) sensed from the current sense resistor ( $R_{CS}$ ), and the valley current loop indirectly controls  $I_{M(-)}$  by an adaptive ZVS control loop inside the controller. The loop identifies the ZVS condition on  $V_{sw}$  every cycle to auto-tune the on time width of  $Q_H$ . However, the second-order resonance waveform of ACF makes the small-signal modeling very difficult. So far, only two complex mathematical models for voltage-mode controlled ACF were discussed, a numerical approach in [9][10] and a high-order average model in [11], so the analytical model for a current-mode controlled ACF still needs further investigation.

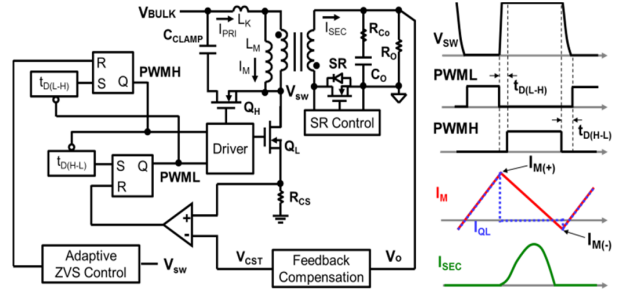


Fig. 1. Hysteresis current mode control of UCC28780 for TM ACF [8]

Once the output load reduces, the light load efficiency becomes very sensitive to the circulating energy needed for ZVS. When the peak current loop reduces  $I_{M(+)}$  to regulate the output power,  $I_{M(+)}$  and  $I_{M(-)}$  become comparable in light load. The increased contribution of the circulating energy impairs the transformer efficiency. The burst mode control improves ACF efficiency, since the ratio of  $I_{M(+)}$  and  $I_{M(-)}$  of each switching cycle in a burst packet can remain higher [12]. The block diagram and operation waveforms of the burst mode control in UCC28780 are shown in Fig. 2. Since  $I_{M(+)}$  is clamped by a fixed peak current threshold ( $V_{CST}$ ),  $V_O$  regulation is achieved by using a ripple regulator to compare the  $V_O$  feedback signal ( $V_{FB}$ ) with the sum of a reference voltage ( $V_{REF}$ ) and a clean compensation ramp ( $V_{COMP}$ ) [8].  $V_{COMP}$  can be used to mitigate the interference of noisy  $V_{FB}$  content onto the intersection point change in steady state. The regulator output ( $RUN$ ) goes high to initiate the next burst cycle when the two signals intersect. The counter limits the maximum number of switching cycles in a burst packet by resetting the  $RUN$  signal.

